Computational Modeling of a Binding Conformation of the Intermediate L-Histidinal to Histidinol Dehydrogenase

Keigo Gohda,*,†,‡ Daisaku Ohta,§,| Genji Iwasaki,‡,§ Peter Ertl,†,^ and Olivier Jacob†,^

Research and Development Department, Crop Protection Division, CIBA-GEIGY AG, Basel CH-4002, Switzerland, International Research Laboratories, CIBA-GEIGY Japan Ltd., P.O. Box 1, Takarazuka, Hyogo 665, Japan, and Research Department, Novartis Crop Protection AG, Basel CH-4002, Switzerland

Received May 26, 2000

Histidinol dehydrogenase (HDH) is one of the enzymes involved in the L-histidine biosynthesis pathway. HDH is a dimer that contains one Zn^{2+} ion in each identical subunit. In this study, we predicted a possible binding conformation of the intermediate L-histidinal, which is experimentally not known, using a computational modeling method and three potent HDH inhibitors whose structures are similar to that of L-histidinal. At first, a set of the most probable active conformations of the potent inhibitors was determined using two different pharmacophore mapping techniques, the active analogue approach and the distance comparison method. From the most probable active conformations of the three potent inhibitors, the common parts of the L-histidinal structure were extracted and refined by energy minimization to obtain the binding conformation of L-histidinal. This predicted conformation of L-histidinal agrees with an experimentally determined conformation of L-histidine in a single crystal, suggesting that it is an experimentally acceptable conformation. The capability in this conformation to coordinate a Zn^{2+} ion was examined by comparing the spatial relative geometry of its functional groups with those of ligands that coordinate with a Zn^{2+} ion in Zn proteins of the Protein Data Bank. This comparison supported our predicted conformation.

INTRODUCTION

Histidinol dehydrogenase (HDH; L-histidinol:NAD oxidoreductase**;** E.C. 1.1.1.23) catalyzes the final steps in the histidine biosynthesis pathway in microbes and plants: the substrate L-histidinol **(1**) is oxidized to a product, L-histidine (**3**), through L-histidinal (**2**) as the intermediate (Scheme 1).[1] This enzyme is a dimer form with an identical subunit, and each contains one Zn^{2+} ion as a cofactor. The metal ion is essential for this catalytic reaction because the enzyme loses its activity after chelation of the metal ion.[2] However, because no crystal structure of HDH has been reported, the coordination of Zn^{2+} with amino acid residues in the enzyme is still unclear. Nevertheless, recent mutation studies[3−5] and NMR[6,7] studies contribute to our understanding of this enzyme. Two conserved cysteine residues in HDH were subjected to replacement by Ala, Ser, or Phe residues in the mutation studies; all the mutant enzymes retained their catalytic activity in each reaction step.[3,4] Conversely, the mutation studies for highly conserved His or Lys residues revealed that the Asn mutant of one of the His residues (the 261st in cabbage HDH) loses Zn^{2+} ligating ability and inactivates the enzyme.[5] These mutation studies suggest that the His residue is involved in the coordination of the metal ion, whereas the Cys residues are not. Recently, Teng and Grubmeyer studied the role of five histidine residues in *Salmonella typhimurium* HDH by mutagenesis; they proposed that His261 and -326 are involved in the catalytic reaction and His261 and -418 are candidates for zinc ion ligands.[8] The ^{113}Cd NMR measurements for HDH containing $^{113}Cd^{2+}$ instead of Zn^{2+} support these observations. Kanaori et al.[6] analyzed the chemical shifts of the ^{113}Cd resonance of the enzyme with or without each of the following: substrates, inhibitors, and NAD^+. The metal ion was then found to coordinate the enzyme with the combination of nitrogen and oxygen ligands that follows the empirical rule for the ^{113}Cd chemical shift on the dependency of ligand species.[9] This combination is most probably two His residues and one Asp or Glu residue in the enzyme. In addition to the identification of the ligand species in the enzyme, Kanaori et al.[6] proposed a possible binding mode of a ligand to the metal by analyzing the ^{113}Cd chemical shift in the holoenzyme state; the nitrogen atom of the imidazole ring and the oxygen atom of the keto

Scheme 1. Reaction Pathway of HDH

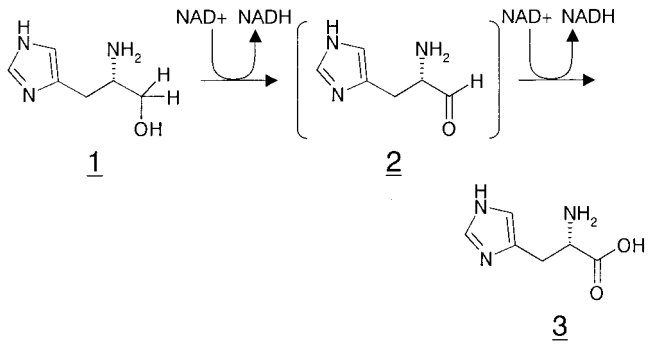

* To whom correspondence should be addressed at Novartis Pharma K. K. Phone: +81-298-65-2252. Fax: +81-298-65-2308. E-mail: keigo.gohda@pharma.novartis.com.
† CIBA-GEIGY AG.
‡ Present address: Research Department, Novartis Pharma K. K., Ohkubo 8, Tsukuba, Ibaraki 300-2611, Japan.
§ CIBA-GEIGY Japan Ltd.
| Present address: College of Agriculture, Osaka Prefectural University, Gakuen-cho, Sakai, Osaka 599-8531, Japan.
^ Novartis Crop Protection AG.

10.1021/ci000332n CCC: $20.00
Published on Web 12/02/2000

Scheme 2. Proposed Binding Model of a Ligand Molecule to the Metal by Kanaori et al.[6] (X = CH_2OH, CHO, COOH, and $COCH_3$)

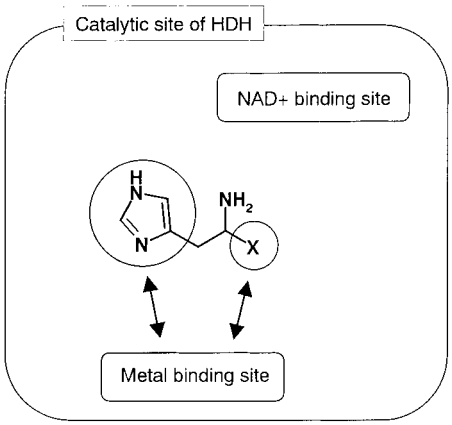

or alcohol group in the substrate or inhibitor of HDH bind to the metal ion, whereas the nitrogen atom of the amine group in the ligand molecule is not involved in the coordination (Scheme 2).

To further understand the metal coordination manner of a ligand molecule in 3D, we computed a possible binding conformation of the intermediate L-histidinal using only knowledge of ligands for the HDH enzyme. This ligand-based prediction was started from determining the most probable active conformations of potent HDH inhibitors, which are chemically and structurally close to L-histidinal, by pharmacophore mapping techniques. Then, the possible binding conformation of L-histidinal was modeled using the most probable active conformations of the potent histidinal-like inhibitors. We used the histidinal-like inhibitors because L-histidinal is known to bind very tightly to HDH.[10,11] The potent HDH inhibitors used in this study were developed in our laboratories. Although several simple chemicals, such as imidazole, histamine, and D-histidine, are known as HDH inhibitors, few SAR studies of HDH inhibitors have been reported.[12] Recently, the AgrEvo group reported a novel type of potent inhibitors that possess an aromatic moiety attached at the position of hydride transfer; this suggests the existence of a lipophilic binding pocket adjoining the active site.[13] Our HDH inhibitors were also in this class. The details of the syntheses of these compounds and the SAR analyses will be described elsewhere. At the end of this paper, the biological relevance of the predicted binding conformation of L-histidinal is discussed by examining the possibility of the predicted binding conformation to coordinate a Zn^{2+} ion compared with the Zn^{2+} coordinating geometries observed in Zn proteins in the Protein Data Bank (PDB).[14]

COMPUTATIONAL METHODS

All modeling and computations were run on an Indigo2 workstation (Silicon Graphics Inc.). The initial structures of the compounds were constructed using the Sketch Molecule function of the SYBYL 6.04 molecular modeling suites (Tripos Inc.). The full geometry optimization and atomic charge calculation were performed using the PM3 method of the MOPAC 5.0 program package with the keyword PRECISE.[15] The Mulliken population analysis was used to obtain partial atomic charges. The conformational energy was calculated using the MaxiMin2 minimizer with the standard

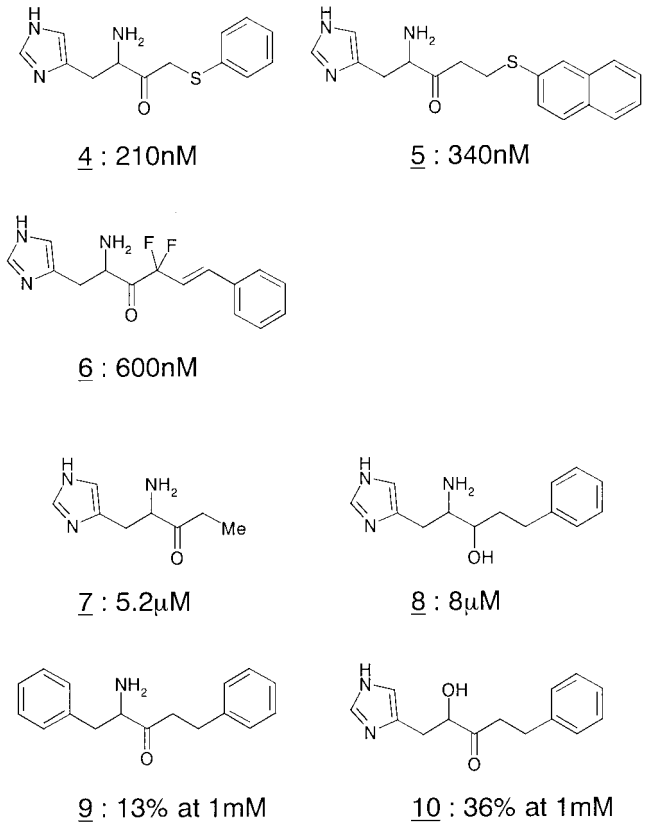

Figure 1. HDH inhibitors with their inhibitory activities (IC_{50}).

Tripos force field, an 8 Å nonbonding cutoff distance, and a distance-dependent dielectric function with $\epsilon = 1$.

The AAA and DISCO analyses were conducted using the Advance Computation and DISCO modules in the SYBYL package. The details of the parameters in each analysis are described in the Results and Discussion. The enzyme inhibitory activity used recombinant cabbage HDH, and was examined by the previously reported assay method.[4,11]

RESULTS AND DISCUSSION

Identification of Pharmacophores. To map the pharmacophores, pharmacophoric groups have to be assumed among the active compounds. Figure 1 shows the HDH inhibitors used in the analyses. Compounds **4**−**6** were defined as potent inhibitors, having IC_{50} values of less than 1 μM. Compounds **7**−**10** were instead defined as weak inhibitors because their IC_{50} values are more than 1 μM. By comparing the chemical structures of the potent and weak inhibitors, a functionality in the inhibitors relevant to their inhibitory activity was elucidated: the activity of compound **7** became weak by removing the terminal hydrophobic group, the activity in compound **8** decreased due to reduction of the carbonyl group, the weak activity of compound **9** demonstrated the importance of the imidazole ring, and replacement of the amino group by a hydroxyl group decreased the activity in compound **10**. In summary, the following four functionalities were identified as pharmacophores relevant to the activity: the imidazole ring, the amino group, the carbonyl group, and the terminal hydrophobic group.

For all the computations, the compounds were assumed neutral. This assumption should be reasonable because there is no experimental data on the pK_a values of either the

imidazole ring or the amino group in ligand molecules in the enzyme complex state; also, recent studies demonstrated that catalytic histidine residues have higher pK_a values (7.9−8.4) than the solution pK_a, suggesting a local pK_a change in the catalytic site of the enzyme.[16,17] Moreover, the imidazole ring is likely deprotonated when coordinating to the Zn^{2+} ion in the enzyme. For the deprotonated state of an imidazole ring, two tautomers can possibly form with a proton on either the N^{δ} or N^{ϵ} position. To model the imidazole structure, the occurrence of each tautomer was analyzed for the crystal structures of histidine-type molecules in the Cambridge Structural Database (CSD).[18] In total, nine single-crystal structures with the deprotonated state of imidazole rings were found in the database with the following CSD reference codes: BALHIS, BALHIS01, DLHIST, LHISTD01, LHISTD02, LHISTD04, LHISTD10, LHISTD13, and JUKMOR. All imidazole rings except for those of JUKMOR had a proton at the N^{ϵ} position. Thus, the imidazole rings of the compounds were tautomerized with a proton at the N^{ϵ} position in all the models.

Pharmacophore Mapping. In the pharmacophore mapping, the three potent inhibitors, compounds **4**−**6**, were used to determine a set of active conformations. Two different pharmacophore mapping techniques were successively employed, namely, the active analogue approach (AAA) and the distance comparison (DISCO) method. The reason for using two different mapping techniques was that one unique set of the most probable active conformations could not be obtained using a single method. This is because the three potent inhibitors contain moderate numbers of free rotatable bonds and all have very similar chemical structures. As a first step, the AAA was used to reduce the number of putative active conformations, and then the DISCO method was used to identify the most probable active conformations.

AAA Analyses. The AAA method is a pharmacophore mapping technique developed by Marshall's group and successfully applied to the study of angiotensin-converting enzyme inhibitors.[19] This method is based on both systematic conformational search and distance map analysis to identify the active conformation among a set of active compounds having different chemical structures.[19−21] For its implementation, we must prepare a set of conformational samples for each active compound and assign internal molecular distances between their pharmacophoric groups. To obtain conformational samples, energetically available conformations were explored by systematically changing the torsion angles of all rotatable bonds.[22] The energetically available conformations do not have to be one of the lowest-energy conformations because an active conformation in an enzyme or a receptor is not necessarily a global or even a local minimum structure. Using the obtained conformational samples and internal molecular distances between the pharmacophoric groups, a multiple dimensional distance map was drawn for each compound. This map represents the available conformational spaces of each compound that are defined by the internal molecular distances. In other words, the obtained map for each compound can be considered as a potential pharmacophoric area because the compound is active. Thus, the intersection among the sets of the pharmacophoric areas leads to identification of the common pharmacophoric areas shared by the active compounds if the active compounds possess a common binding mode in the complex. The energetically available conformations within the common areas can then be defined as a set of active conformations.

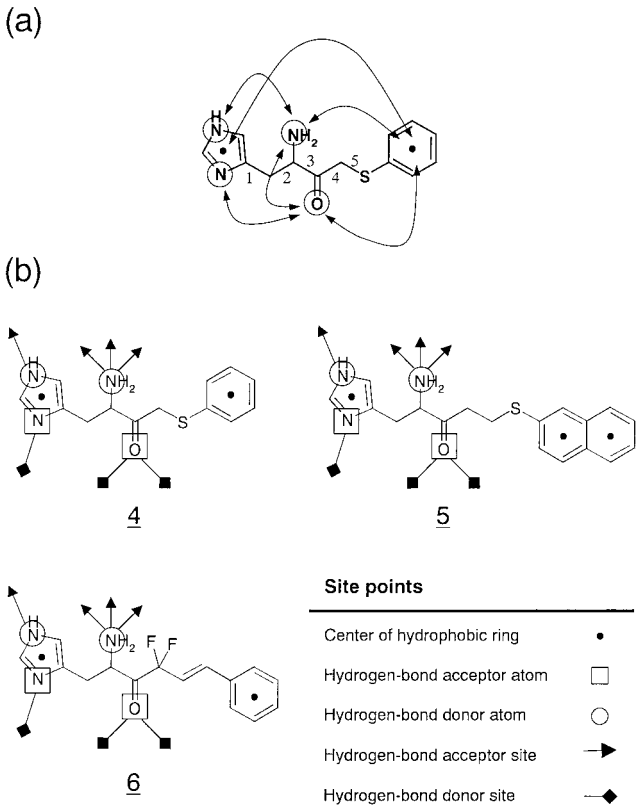

Figure 2. (a) Pharmacophores (open and closed circles) and interpharmacophoric distances (lines with arrowheads) for the active analogue approach. Arabic numbers indicate the rotatable bonds used in the cluster analysis. An example for compound **4** is shown. (b) Site points in the pharmacophores used in the DISCO method.

In this study, a systematic conformational search for the three potent inhibitors was done by changing all the rotatable bonds in the molecules by 30° increments on the torsion angles (vdW factor 0.95 and grid space 0.1 Å), and thus generating 10^{12-13} energetically available conformations for each compound. On the basis of the four pharmacophoric groups, six internal molecular distances to represent pharmacophoric areas were assigned as shown in Figure 2a. Using the conformational samples and the internal distances, the pharmacophoric areas were created for each compound, and then intersected with each other to get the potential pharmacophoric areas. As a result of the intersections, the number of energetically available conformations for each compound decreased from 10^{12-13} to 461 conformations for compound **4**, 491 conformations for compound **5**, and 185 conformations for compound **6**. These conformations were next classified using the cluster analysis according to the torsion angles shown in Figure 2a. For compound **5**, six torsion angles were used. A unique cluster was defined as the group of conformers with common torsion angle values in a range of ±30° for every torsion bond. The lowest-energy conformer in each cluster was used as a representative conformation. This classification reduced the number of conformations to 19 for compound **4**, 23 for compound **5**, and 14 for compound **6**. This set of putative active conformations was used for the following DISCO analyses as a set of representative conformations.

DISCO Analyses. The DISCO method superimposes the pharmacophore of representative conformations among active compounds to obtain the active conformations,[23] and has been used for identifying bioactive conformations or possible pharmacophores.[24−28] The pharmacophore used in the DISCO method includes both the atomic positions of functional groups and the putative receptor sites of hydrogen-bond acceptors and donors. It can also include the center positions of charged groups and hydrophobic groups. These site points are defined on the basis of the geometry of heavy atoms.

The flow of the DISCO method is the following: First, a conformational sampling of each compound is done to obtain a set of representative conformations. Then, the pharmacophoric site points are assigned to all the representative conformations. With the set of conformations and site points among the active compounds, the preferable conformational combinations among the compounds are searched by superimposing on common pharmacophoric site points. Finally, among the remaining combinations, the most probable active conformation for each compound is determined by considering several criteria for the goodness of the conformational combination: the number of matched site points, the distance tolerance between the site points, the root-mean-square values of the overlap, and the conformational energy of conformation.

For the analyses, 13 or 14 site points were defined as the pharmacophore for each compound (Figure 2b). Two hydrogen-bond acceptor atoms and two hydrogen-bond donor atoms were used as atomic site points. The receptor site points were built by adding dummy atoms with a 3 Å bond length from the hydrogen-bond acceptor or donor atoms. Three hydrogen-bond acceptor receptor sites were placed on the nitrogen atom of the amino group in a trihedral shape. One hydrogen-bond acceptor receptor site and one hydrogen-bond donor receptor site were built on the imidazole ring. Two hydrogen-bond donor receptor sites were placed in the plane of the carbonyl group with a 120° bond angle. One site point was put in the center of the imidazole ring, and one or two points were for the center of the hydrophobic rings. The construction of all site points followed the standard procedure of the DISCO method. Using the defined site points and a few tens of the putative active conformations for each compound obtained from the AAA analyses, enumerative superpositions by the DISCO method were conducted with the following criteria: the site points must match more than 10 points within the distance tolerances of 0.6 Å. Compound **4** was used as a template for the DISCO analysis because it was the most active compound among the three inhibitors. As a result of the superposition, the best set of conformational combinations for each compound was obtained (Figure 3). Each conformation had 11 site point matches and a low conformational energy (Table 1). The distance tolerances between the compounds were 0.31 Å for compound 5 and 0.40 Å for compound **6**. The larger number of site point matches and the small value of the tolerances indicate that the obtained set of conformations are the most probable active conformations. As seen in Figure 3, all three compounds adopted "extend conformations". The moieties of histidinal in the compounds superimposed on each other very closely. Conversely, the overlapping of the terminal hydrophobic groups was not good. This could be due to variations in the linkers among the compounds between the histidinal moiety and the hydrophobic group, for instance, chain-length differences and conformational constraints. The position of the second phenyl moiety of compound **5** was not in an overlapping area. Because compound **5** still retains a potent inhibitory activity, this suggests that the enzyme might have a larger hydrophobic pocket around this site; however, the biological relevance of the pocket remains to be clarified. As the second best superposition, the DISCO provided "bend conformations" (data not shown). For the bend conformations, the site point match was 10 points and their conformational energy values were larger than those of the extend conformations.

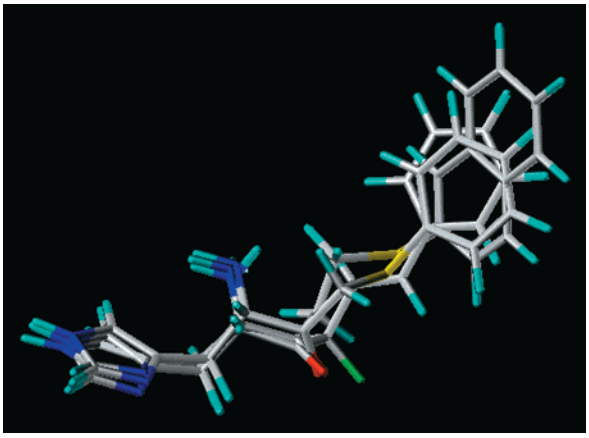

Figure 3. DISCO model of compounds **4**−**6**.

Table 1. Details of the DISCO Model

compd	fit (Å^2)	overlap (Å^3)	tolerance (Å)	E (kcal/mol)
4	0.00	234.1	0.00	2.7
5	0.40	145.3	0.31	7.1
6	0.50	155.8	0.40	2.4

Modeling the Binding Conformation of L-Histidinal. The intermediate in the whole HDH reaction is L-histidinal. Using the most probable active conformations of the potent inhibitors, we modeled its binding conformation as follows. First, the fragments common to the L-histidinal structure were separately extracted from the most probable active conformations of each compound, and then the coordinates of these three fragments were averaged. Second, a hydrogen atom was attached to the position of the aldehyde group in the averaged fragment. This was our initial model of L-histidinal. The energy minimization for all hydrogen atoms of the initial model was then done while the positions of the heavy atoms were fixed. Then, the positions of both heavy atoms and hydrogen atoms were energetically relaxed while the overall conformation of the initial model was kept by constraining the torsion angles of all rotatable bonds (constraint weight 100.0 kcal/mol). As a result, the binding conformation of L-histidinal shown in Figure 4 was obtained. To examine the conformational acceptability of this predicted L-histidinal conformation, it was compared with the seven crystal structures in the CSD used for the assignment of the imidazole ring tautomerization (except a structure in BALHIS that is a D-configuration). As a result, the structure in DLHIST with a L-histidine molecule overlapped very well with the predicted L-histidinal conformation; its root-mean-square deviation (RMSD) was 0.137 Å, whereas the average RMSD value of the other comparisons was 1.081 Å (Table

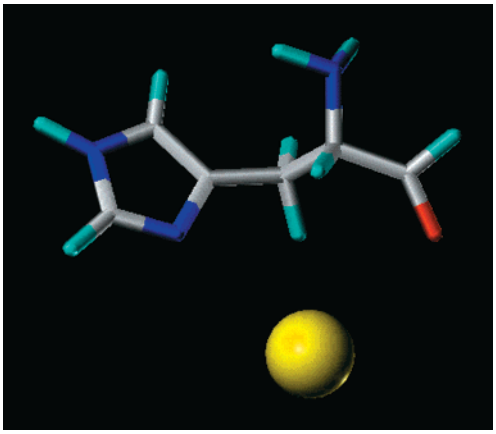

Figure 4. A possible binding conformation of L-histidinal to HDH. The yellow sphere represents the position of a Zn^{2+} ion potentially coordinating with L-histidinal.

Table 2. Structural Comparison of Predicted Histidinal with Crystal Structures in CSD

molecule	RMSD (Å)	χ^1 (deg)[a]	χ^2 (deg)[a]
pred histidinal	0.000	−81.2	−78.8
BALHIS01	1.042	−178.7	62.2
DLHIST	0.137	−86.7	−68.1
LHISTD01	1.084	−57.8	53.2
LHISTD02	1.095	−62.2	58.0
LHISTD04	1.077	−58.5	54.0
LHISTD10	1.093	−59.2	56.8
LHISTD13	1.096	−58.4	56.6

[a] χ angles were defined as follows: χ^1 = (N atom of the amino group)−C^α−C^β−C^γ and $\chi^2 = C^\alpha - C^\beta - C^\gamma - N^\delta$.

2). The conformational differences were mainly from differences of the χ^2 angle. The structural agreement with a molecule in a single crystal suggested that the predicted conformation of L-histidinal is likely to be experimentally acceptable.

In the L-histidinal conformation, the N^δ atom of the imidazole ring and oxygen atom of the carbonyl group were directed on the same side, suggesting the capability to coordinate with a Zn^{2+} ion in the enzyme. Also, we found that the amino group was oriented toward the opposite side of the imidazole−carbonyl face. This qualitatively agrees with the ^{113}Cd NMR proposed metal-binding model (Scheme 2).[6]

CONCLUSIONS

Biological Implications. We reported herein a computational prediction of the possible binding conformation of L-histidinal to HDH using the ligand-based approach with the assumption that a potent inhibitor should bind tightly to the enzyme with a conformation similar to that of the intermediate. As reported in the ^{113}Cd NMR study, ligand molecules, i.e., substrates and inhibitors, can bind to the metal ion with or without NAD^+, and the structure around the active site in the binary complex HDH−inhibitor remains unchanged by the binding of NAD^+.[6] Therefore, the geometrical capability to Zn^{2+} coordination should be a necessary requirement for the L-histidinal conformation in the active site. To evaluate the predicted L-histidinal binding conformation, we demonstrated its capability of Zn^{2+} coordination by comparison to the Zn^{2+} coordination geometry observed in Zn proteins complexed with ligand molecules.

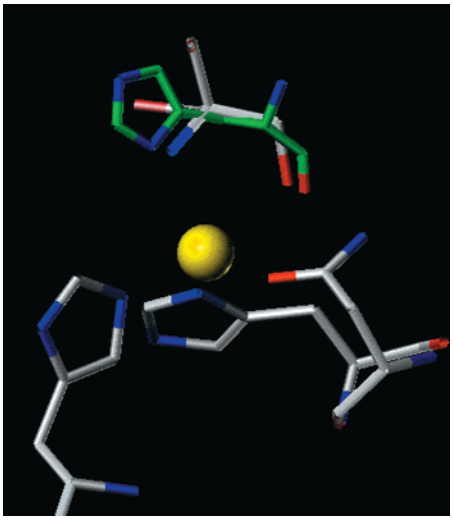

Figure 5. L-Histidinal coordination model superimposed on the Zn^{2+} binding site of carbonic anhydrase II that is complexed with tromethamine (1H4N). The structure of L-histidinal is green, and the Zn^{2+} ion is yellow. The positions of the Zn^{2+} ion and two coordinating atoms in each ligand molecule were used for the superpositioning. All hydrogen atoms are omitted for clarification.

For the analyses, crystal structures of Zn^{2+} coordinating proteins with resolution below 2.5 Å were used. In total, 443 entries were found in the PDB. In the entries, all complexes having a cysteine residue as a coordination ligand were excluded because the mutation[3,4] and ^{113}Cd NMR studies[6] demonstrated that no cysteine residue is involved in the metal coordination in HDH. Also all entries with no ligand molecule coordinating to the metal ion were excluded. Seventy entries[29] out of 443 fulfilled these criteria. The intermolecular distances and the coordination-bond angles between the metal and ligand molecule were analyzed in the 70 complexes. The results are summarized as follows: the average distance for Zn coordination is 2.24 ± 0.28 Å, and the average bond angle is 74.6 ± 5.2°.

Using this information, the possibility of Zn^{2+} coordination for the predicted L-histidinal binding conformation was examined by visually inspecting the position of a Zn^{2+} ion. Then, we found that the metal ion can be placed with the proper geometry to form coordination with the L-histidinal. Shown in Figure 4 is one possible coordination model; in this model, the intermolecular distances and the coordination-bond angle among Zn^{2+}, the N^δ atom of the imidazole ring, and the oxygen atom of the carbonyl group are 2.56 Å, 2.56 Å, and 88.2°, respectively. The geometry of this predicted Zn^{2+} coordination agrees with the experimental Zn^{2+} coordination geometry. In addition, one example of superimposing the coordination model with the Zn^{2+} binding site of a protein structure is shown in Figure 5. The protein structure is the Zn^{2+} binding site of carbonic anhydrase II complexed with a ligand molecule tromethamine (PDB code 1H4N). Carbonic anhydrase II contains two nitrogens from His and one oxygen from Asn side chains in the enzyme as the Zn^{2+} coordination ligand combination, which is similar to our proposed coordination manner for HDH. In the complex, the tromethamine is coordinated to a Zn^{2+} ion with the amine and hydroxyl groups. In the superimposed picture, the skeleton part of the L-histidinal conformation overlapped very

well spatially onto that of tromethamine; the positions of the atoms involved in Zn^{2+} coordination also overlap very closely (Figure 5).

This evidence that the L-histidinal binding conformation computationally modeled by the ligand-based prediction approach, without experimental data on the conformation, agrees with the structural features experimentally determined by the ^{113}Cd NMR and crystallographic analyses leads to the conclusion that the predicted L-histidinal conformation in this study is likely biologically relevant to the binding to the HDH enzyme. Using this knowledge of the L-histidinal binding conformation, we next plan to develop a more potent HDH inhibitor by either fixing a conformation similar to the binding conformation or seeking various chelating functionalities to the metal ion.

ACKNOWLEDGMENT

We gratefully thank Dr. K. Kanaori for many helpful discussions.

REFERENCES AND NOTES

(1) Adams, E. L-Histidinal, a biosynthetic precursor of histidine. *J. Biol. Chem.* **1955**, *217*, 325−344.
(2) Lee, S. Y.; Grubmeyer, C. T. Purification and in vitro complementation of mutant histidinol dehydrogenases. *J. Bacteriol.* **1987**, *169*, 3938−3944.
(3) Teng, H.; Segura, E.; Grubmeyer, C. Conserved cysteine residues of histidinol dehydrogenase are not involved in catalysis. *J. Biol. Chem.* **1993**, *268*, 14182−14188.
(4) Nagai, A.; Kheirolomoom, A.; Ohta, D. Site-directed mutagenesis shows that the conserved cysteine residues of histidinol dehydrogenase are not essential for catalysis. *J. Biochem.* **1993**, *114*, 856−861.
(5) Nagai, A.; Ohta, D. Histidinol dehydrogenase loses its catalytic function through the mutation of $His^{261} \rightarrow$ Asn due to its inability to ligate the essential Zn. *J. Biochem.* **1994**, *115*, 22−25.
(6) Kanaori, K.; Uodome, N.; Nagai, A.; Ohta, D.; Ogawa, A.; Iwasaki, G.; Nosaka, A. Y. ^{113}Cd nuclear magnetic resonance studies of cabbage histidinol dehydrogenase. *Biochemistry* **1996**, *35*, 5949−5954.
(7) Kanaori, K.; Ohta, D.; Nosaka, A. Y. Effects of excess cadmium ion on the metal binding site of cabbage histidinol dehydrogenase studies by ^{113}Cd-NMR spectroscopy. *FEBS Lett.* **1997**, *412*, 301−304.
(8) Teng, H.; Grubmeyer, C. Mutagenesis of histidinol dehydrogenase reveals roles for conserved histidine residues. *Biochemistry* **1999**, *38*, 7363−7371.
(9) Summers, M. F. Cadmium-113 NMR spectroscopy of coordination compounds and proteins. *Coord. Chem. Rev.* **1988**, *86*, 43−134.
(10) Gorisch, H.; Holke, W. Binding of histidinal to histidinol dehydrogenase. *Eur. J. Biochem.* **1985**, *150*, 305−308.
(11) Kheirolomoom, A.; Mano, J.; Nagai, A.; Ogawa, A.; Iwasaki, G.; Ohta, D. Steady-state kinetics of cabbage histidinol dehydrogenase. *Arch. Biochem. Biophys.* **1994**, *312*, 493−500.
(12) Grubmeyer, C. T.; Insinga, S.; Bhatia, M.; Moazami, N. *Salmonella typhimurium* histidinol dehydrogenase: complete reaction stereochemistry and active site mapping. *Biochemistry* **1989**, *28*, 8174−8180.
(13) Dancer, J.E.; Ford, M. J.; Hamilton, K.; Kilkelly, M.; Lindell, S. D.; O'Mahony, M. J.; Saville-Stones, E. A. Synthesis of potent inhibitors of histidinol dehydrogenase. *Bioorg. Med. Chem. Lett.* **1996**, *6*, 2131−2136.
(14) Bernstein, F. C.; Koetzle, T. F.; Williams, G. J. B.; Meyer Jr, E. F.; Brice, M. D.; Rodgers, J. R.; Kennard, O.; Simanouchi, T.; Tasumi, M. The Protein Data Bank: a computer-based archival file for macromolecular structures. *J. Mol. Biol.* **1977**, *112*, 535−542.
(15) Stewart, J. J. P. Optimization of parameters for semiempirical methods. I. Method. *J. Comput. Chem.* **1989**, *10*, 209−220.
(16) Grubmeyer, C.; Teng, H. Mechanism of *Salmonella typhimurium* histidinol dehydrogenase: kinetic isotope effects and pH profiles. *Biochemistry* **1999**, *38*, 7355−7362.
(17) Fersht, A. *Enzyme structure and mechanism*, 2nd ed.; W.H. Freeman and Co.: New York, 1985; pp 155−175.
(18) Allen, F. H.; Bellard, S.; Brice, M. D.; Cartwright, B.A.; Doubleday: A.; Higgs, H.; Hummelink, T.; Hummelink-Peter, B. G.; Kennard, O.; Motherwell, W. D. S.; Rodgers, J. R.; Watson, D. G. The Cambridge Crystallographic Data Centre: computer-based search, retrieval, analysis and display of information. *Acta Crystallogr.* **1979**, *B35*, 2331−2339.
(19) Mayer, D.; Naylor, C. B.; Motoc, I.; Marshall, G. R. A unique geometry of the active site of angiotensin-converting enzyme consistent with structure−activity studies. *J. Comput.-Aided Mol. Des.* **1987**, *1*, 3−16.
(20) Marshall, G. R.; Barry, C. D.; Bosshard, H. E.; Dammkoehler, R. A.; Dunn, D. A. In *Computer-Assisted Drug Design*; Olsen, E. C., Christoffersen, R. E., Eds.; American Chemical Society: Washington, DC, 1979; pp 205−226.
(21) Depriest, S. A.; Mayer, D.; Naylor, C. B.; Marshall, G. R. 3D-QSAR of angiotensin-converting enzyme and thermolysin inhibitors: a comparison of CoMFA models based on deduced and experimentally determined active site geometries. *J. Am. Chem. Soc.* **1993**, *115*, 5372−5384.
(22) Motoc, I.; Dammkoehler, R. A.; Mayer, D.; Labanowski, J. Three-dimensional quantitative structure−activity relationships. I. General approach to the pharmacophore model validation. *Quant. Struct.-Act. Relat.* **1986**, *5*, 99−105.
(23) Martin, Y. C.; Bures, M. G.; Danaher, E. A.; DeLazzer, J.; Lico, I.; Pavlik, P. A. A fast new approach to pharmacophore mapping and its application to dopaminergic and benzodiazepine agonists. *J. Comput.-Aided Mol. Des.* **1993**, *7*, 83−102.
(24) Myers, A. M.; Charifson, P. S.; Owens, C. E.; Kula, N. S.; McPhail, A. T.; Baldessarini, R. J.; Booth, R. G.; Wyrick, S. D. Conformational analysis, pharmacophore identification, and comparative molecular field analysis of ligands for the neuromodulatory σ_3 receptor. *J. Med. Chem.* **1994**, *37*, 4109−4117.
(25) Goldstein, S.; Neuwels, M.; Moureau, F.; Berckmans, D.; Lassoie, M. A.; Differding, E.; Houssin, R.; Henichart, J. P. Bioactive conformations of peptides and mimetics as milestones in drug design: investigation of NK_1 receptor antagonists. *Lett. Pept. Sci.* **1995**, *2*, 125−134.
(26) Spadoni, G.; Balsamini, C.; Diamantini, G.; Giacomo, B. D.; Tarzia, G.; Mor, M.; Plazzi, P. V.; Rivara, S.; Lucini, V.; Nonno, R.; Pannacci, M.; Fraschini, F.; Stankov, B. M. Conformationally restricted melatonin analogues: synthesis, binding affinity for the melatonin receptor, evaluation of the biological activity, and molecular modeling study. *J. Med. Chem.* **1997**, *40*, 1990−2002.
(27) Fossa, P.; Boggia, R.; Mosti, L. Toward the identification of the cardiac cGMP inhibited-phosphodiesterase catalytic site. *J. Comput.-Aided Mol. Des.* **1998**, *12*, 361−372.
(28) Matyus, P.; Borosy, A. P.; Varro, A.; Papp, J. G.; Barlocco, D.; Cignarella, G. Development of pharmacophores for inhibitors of the rapid component of the cardiac delayed rectifier potassium current. *Int. J. Quantum Chem.* **1998**, *69*, 21−30.
(29) The PDB codes of the 70 entries used in the analysis are the following: 1A42, 1A4M, 1AF0, 1AK0, 1AM6, 1ATL, 1AVN, 1AZM, 1BCD, 1BNV, 1BV3, 1BZM, 1CBX, 1CIL, 1CIM, 1CIN, 1CNW, 1CNX, 1CNY, 1CPS, 1CRA, 1CVA, 1CZM, 1DMY, 1DTH, 1FRP, 1H4N, 1HCB, 1HFC, 1HFS, 1HYT, 1IGB, 1JAN, 1JAO, 1JAP, 1JAQ, 1KBC, 1KOP, 1LAN, 1LCP, 1MMB, 1MMP, 1MMQ, 1MMR, 1MNC, 1OKL, 1OKM, 1OKN, 1RAY, 1SLN, 1THL, 1TLP, 1TMN, 1UIO, 1XUF, 1XUG, 1XUJ, 1YDB, 1YDD, 1ZSB, 2H4H, 2TCL, 2TMN, 2USN, 4TLN, 4TMN, 5TLN, 5TMN, 6TMN, and 7TLN.

CI000332N